



Düzce University Journal of Science & Technology

Research Article

Investigation of Low Velocity Impact Behavior of Aluminum Honeycomb Sandwich Structures with GFRP Face Sheets by Finite Element Method

 Ilyas BOZKURT *

Department of Mechanical Engineering, Architecture and Engineering Faculty,
Mus Alparslan University, 49250 Mus, Turkey.

*Corresponding author's e-mail address: i.bozkurt@alparslan.edu.tr

DOI: 10.29130/dubited.1477434

ABSTRACT

The aim of this study is to examine the low velocity impact behavior of aluminum honeycomb sandwich structures with glass fiber reinforced plastic (GFRP) face sheets with the help of finite element method. In the study, low velocity impact tests were carried out in the *LS DYNA* finite element program to examine the effects of face sheets thickness, core number, wall thickness, impact location and impact velocity on maximum contact force, absorbed energy efficiency and damage mode. Progressive damage analysis based on the *Hashin damage criterion* and the combination of *Cohesive Zone Model (CZM)* and the bilinear traction-separation law was performed using the *MAT-54* material model. At the end of the study, it was determined that the face sheets thickness in sandwich structures had a significant effect on the impact resistance up to a certain impact energy. It has been observed that as the impact velocity gradually increases, there is a decrease in the contact force after a certain threshold value. As the impactor velocity increases, the energy absorption efficiency also increases. It has been determined that the location of the impact is very effective on peak force and energy absorption efficiency. The effect of the number of core layers depends on the face sheets thickness. When the face sheets thickness was not damaged at first contact, the peak force value increased in parallel with the number of layers. It was determined that the dominant damage mode after impact was matrix damage. It has been observed that as the energy level of the impactor increases, damage also occurs on the back surfaces.

Keywords: Sandwich Composite, Impact test, Progressive damage analysis, Finite element method, Cohesive Zone Model (CZM)

GFRP Yüzeyli Alüminyum Petek Sandviç Yapıların Düşük Hızlı Darbe Davranışlarının Sonlu Elemanlar Yöntemi ile İncelenmesi

ÖZET

Bu çalışmanın amacı cam fiber takviyeli plastik (GFRP) yüzey tabakalı alüminyum petek sandviç yapıların düşük hızlı darbe davranışlarını sonlu elemanlar yöntemi ile incelemektir. Çalışmada plaka kalınlığının, çekirdek katman sayısının, duvar kalınlığının, darbe konumunun ve darbe hızının maksimum temas kuvveti, darbe enerjisi emilimi ve hasar modu üzerindeki etkilerini incelemek için düşük hızlı darbe testleri *LS DYNA* sonlu elemanlar programında gerçekleştirilmiştir. MAT-54

malzeme modeli kullanılarak *Hashin Hasar Kriteri ve Kohezif Bölge Modeli (CZM)* ile çift doğrusal çekiş-ayırma yasasının kombinasyonuna dayalı ilerlemeli hasar analizi gerçekleştirilmiştir. Çalışma sonunda sandviç yapılarda kapak kalınlığının darbe direnci üzerinde belirli bir darbe enerjisine kadar önemli bir etkiye sahip olduğu belirlenmiştir. Darbe hızı kademeli bir şekilde arttıkça belirli bir eşik değerinden sonra temas kuvvetinde düşüşün meydana geldiği belirlenmiştir. Vurucu hızı arttıkça enerji absorbe verimliliği de artmaktadır. Darbenin konumu maksimum kuvvet ve enerji absorbe verimliliği üzerinde çok etkili olduğu belirlenmiştir. Çekirdek katman sayısının etkisi kapak kalınlığına bağlıdır. Kapak kalınlığı ilk temas durumunda hasar almadığı zaman katman sayısı ile paralel olarak peak force değerinin arttığı belirlenmiştir. Darbeden sonra baskın hasar modunun matris hasarı olduğu belirlenmiştir. Vurucunun enerji seviyesi arttıkça arka yüzeylerde de hasarların meydana geldiği görülmüştür.

Anahtar Kelimeler: *Sandviç Kompozit, Darbe testi, İlerlemeli hasar analizi, Sonlu elemanlar yöntemi, Kohezif Bölge Modeli (CZM)*

I. INTRODUCTION

Composite materials are used in many sectors, especially the defense industry, due to their high strength/weight ratio and excellent energy absorption capacity [1]. Sandwich composite structures come to the fore especially in parts and components where energy absorbing properties are needed. Sandwich structures are structures consisting of surfaces such as carbon or glass composites and cores of different shapes and materials (lattice structures, prismatic structures, honeycomb) [2]. Due to the superior properties of sandwich composites, they can be used in many different areas and components and be exposed to many different loading conditions. However, sandwich composites are sensitive to impact damage due to the complexity of the micromechanical structures and the energy absorption system under load [3]. Damages inside the structure that cannot be seen directly affect the rigidity and lifespan of the structure. Therefore, determining the impact behavior of these structures and obtaining detailed information about the damage mechanisms are of great importance for safety [4].

In metal materials, the behavior of the material in case of loading can be predicted with high accuracy due to linearity. However, it is very difficult to determine these behaviors and reactions in composite structures. For this, many tests and analyzes may need to be carried out in a laboratory environment with expensive materials and test equipment. Because there are many components in composite structures. In addition to these, it requires serious calculation and analysis to determine mechanical properties along with structural differences [5].

There are many studies in the literature on the impact performance of composite structures [6-8]. However, many studies examining the performance of sandwich composite structures under load have been conducted by researchers [[2],[4],[9]-[14]]. In these studies, the approach of examining the performance of the sandwich structure under load and determining the structure that will provide optimum performance is generally dominant. Because in sandwich structures, the effect on impact performance can be determined by changing many parameters such as cell and face sheet thickness, honeycomb height, honeycomb geometries. For example, Foo et al. [15] examined the effects of aluminum cell size on impact in sandwich composite structures. At the end of the study, they determined that honeycomb density is an effective parameter on impact. Li et al [9] and Li et al. [16] studied the dynamic behavior of cell size in aluminum honeycomb sandwich panels under air blast loading. Crupi et al. [17] examined the effects of structural changes on the impact behavior of aluminum honeycomb sandwich structures. At the end of the study, they determined that cell sizes in honeycomb structures are very effective on impact performance. He et al [[18], [19]] examined the effect of structural changes on the impact behavior of X-type sandwiches consisting of a carbon fiber-reinforced polymer face sheets and an aluminum alloy core. Albayrak et al. [[21],[22]] examined the impact behavior of curved sandwich composites by adding Ethylene Propylene Diene Monomer (EPDM) rubber interlayers between glass fiber woven fabrics. He et al. [23]

experimentally and numerically investigated the low-velocity impact behavior and damage forms of aluminum honeycomb sandwich structures with carbon fiber reinforced plastic (CFRP) face sheets. Xue et al. [24] examined the impact performances of nomex honeycomb core carbon/glass fiber hybrid composite face sheets sandwich structure for different structural dimensions.

In this study, the low velocity impact behavior of aluminum honeycomb sandwich structures with glass fiber reinforced plastic (GFRP) face sheets was examined with the help of the finite element method. In the study, low velocity impact tests were carried out in the *LS DYNA* finite element program to examine the effects of face sheets thickness, core layer number, wall thickness, impactor location and impact velocity on maximum contact force, absorbed energy efficiency and damage mode. To determine the damage that will occur due to impact, analysis was carried out using the *MAT-54* material model, which provides progressive damage analysis. The strength effects of the parameters examined in the study were determined and the absorbed energy efficiency was compared with studies in the literature.

II. MATERIALS AND METHOD

A.1. Finite Element Model

Dimension details of sandwich composite specimens with aluminum core and glass fiber composite face sheets are given in Figure 1 and Table 1. Low velocity impact test was applied to these specimens, whose dimensions were given. In this study, the change effects of the parameters most studied in the literature were examined. In the impact test, different types of impact loading may occur depending on the velocity of the impactor. If the impact velocity is less than 10 m/s, it is called low-velocity impact, and if it is between 10 m/s and 50 m/s, it is called medium-velocity impact. If the impact velocity is between 50 m/s and 1000 m/s, it is called high-velocity impact [25]. In this study, low-velocity impact tests were applied since the velocity of the impactor was less than 10 m/s.

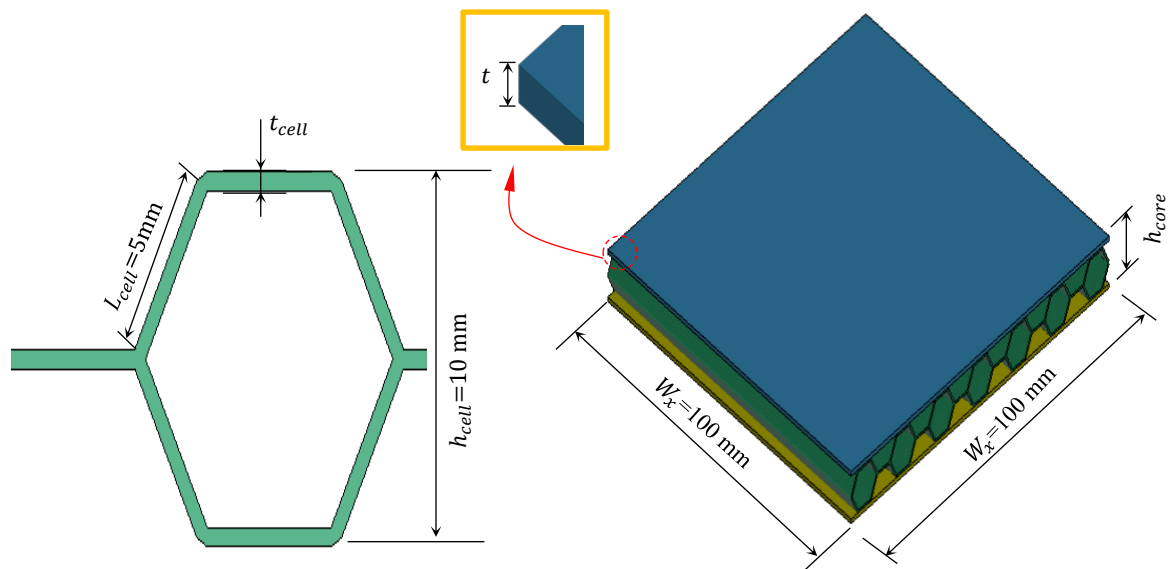


Figure 1: Specimen dimensions.

Table 1. Parameters examined for sandwich panels in impact testing.

No	Face sheet thickness, (t) mm	Cell wall thickness, (t _c) mm	Core number, (n)	Impact Velocity, V (m/s)
1	0.5	0.5	1	3
2	0.5	0.5	1	5
3	0.5	0.5	1	7
4	1	0.5	1	3
5	1	0.5	1	5
6	1	0.5	1	7
7	1.5	0.5	1	3
8	1.5	0.5	1	5
9	1.5	0.5	1	7
10	3	0.5	1	3
11	3	0.5	1	5
12	3	0.5	1	7
13	0.5	1	1	5
14	0.5	2	1	5
15	3	1	1	5
16	3	2	1	5
17	0.5	0.5	2	5
18	0.5	0.5	3	5
19	3	0.5	2	5
20	3	0.5	3	5

In low-velocity impact tests, many graphs and data about the mechanical performance of the material are obtained. In these graphics and outputs, it is decided whether the material is suitable for the component or location to be used or not by comparing it with the standards. In the low velocity experimental test setup, these data are obtained by reading from the impactor tip. Displacement graphs are derived from the impactor 's position along with changes in kinetic energy and velocity. Equations (1)-(4) were used to obtain the changes in velocity, displacement, and energy based on the impact timing. Data regarding the contact force, displacement and absorbed energy obtained from the impactor tip were evaluated.

$$v(t) = v_i + gt - \int_0^t \frac{F(t)}{m} dt \quad (1)$$

Here, t is the time of the first contact of the impactor to the specimen, which is $t = 0$; $v(t)$ is the velocity of the impactor at time t ; v_i is the velocity of the impactor at time $t = 0$; and $F(t)$ is the impact contact force measured at time t .

$$\delta(t) = \delta_i + v_i t + \frac{gt^2}{2} - \int_0^t \left(\int_0^t \frac{F(t)}{m} dt \right) dt \quad (2)$$

δ is the displacement of the striker.

$$E_a(t) = \frac{m(v_i^2 - (v(t))^2)}{2} + mh\delta(t) \quad (3)$$

Here, $E_a(t)$ is the absorbed energy, m is the weight impact, and g is the gravitational acceleration. Divide the weight value to find the specific energy absorption.

$$SEA = \frac{E_a}{m} \quad (4)$$

Here, m is the mass of the specimens. Higher SEA values indicate better energy-absorbing efficiency of the structures.

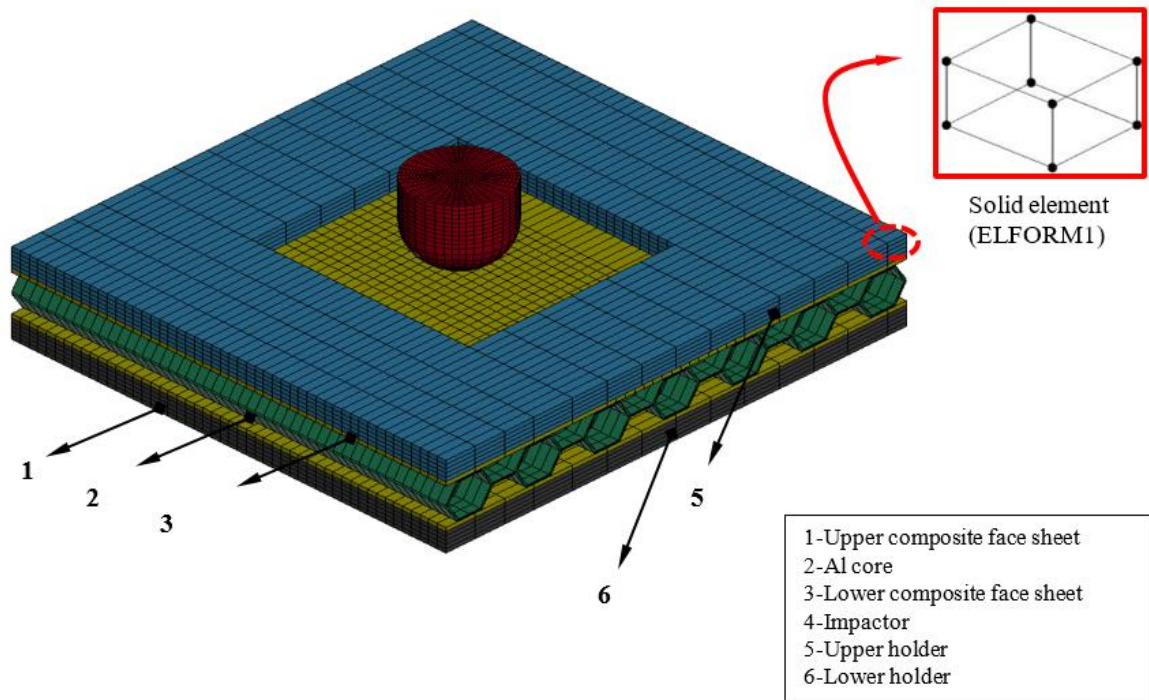


Figure 2. Finite element model of low velocity impact test.

Many finite element programs have been developed to determine the impact behavior of aluminum honeycomb glass sandwich specimens. Among these, *LS-DYNA*, a commercial finite element software program, was preferred due to its wide material library, ease of use of interfaces and the ability to develop complex numerical models [26]. The program's solution methodology includes material cards that provide damage models based on the *Continuous Damage Mechanism* (CDM). It allows structural damage to be visualized in a phased manner using models based on CDM. Impact tests with dimensions of 100x100 mm were carried out numerically for all specimens used in this research. The sandwich composite plate and the upper and lower holders are modeled as shown in Figure 2.

Sandwich composite structures may face different impact loading depending on their usage areas and the components they use. Knowing the magnitude of the impact and the points where the impact occurs is important to understand the reaction of the material. Many different scenarios may occur at the points where the impact will occur. However, since honeycomb core sandwich structures are formed by the formation of a regular hexagonal shape, all possible scenarios can be easily determined by considering certain points here. For this study, the impact was made using the impact performance at three different points shown in Figure 3 as reference. An example impactor point location for P1 is shown in Figure 4.

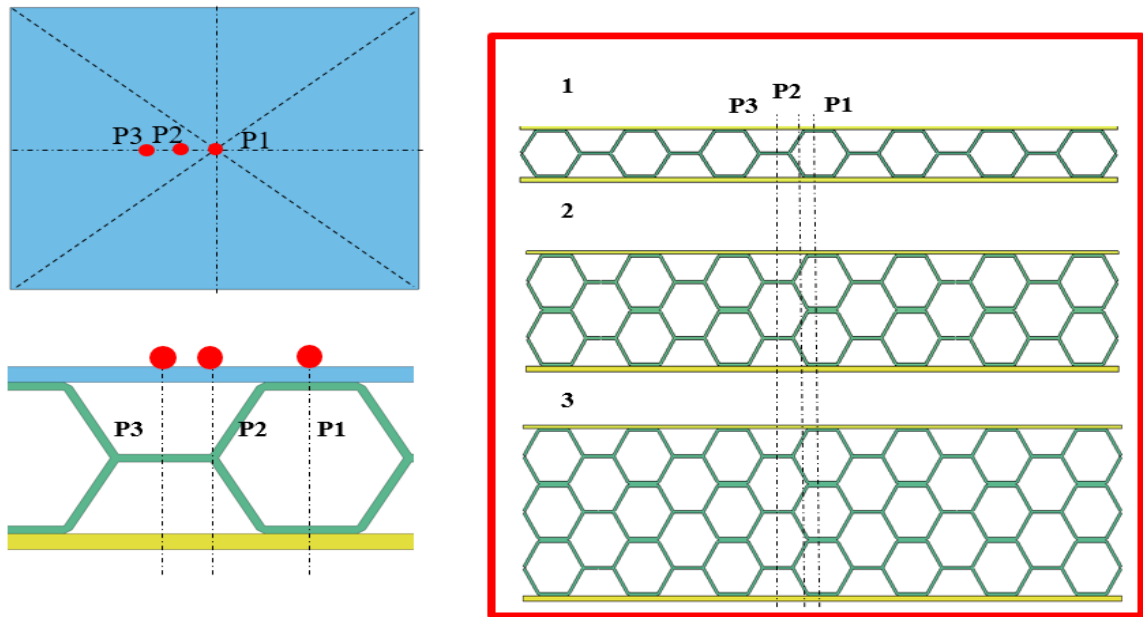


Figure 3. Impact points.

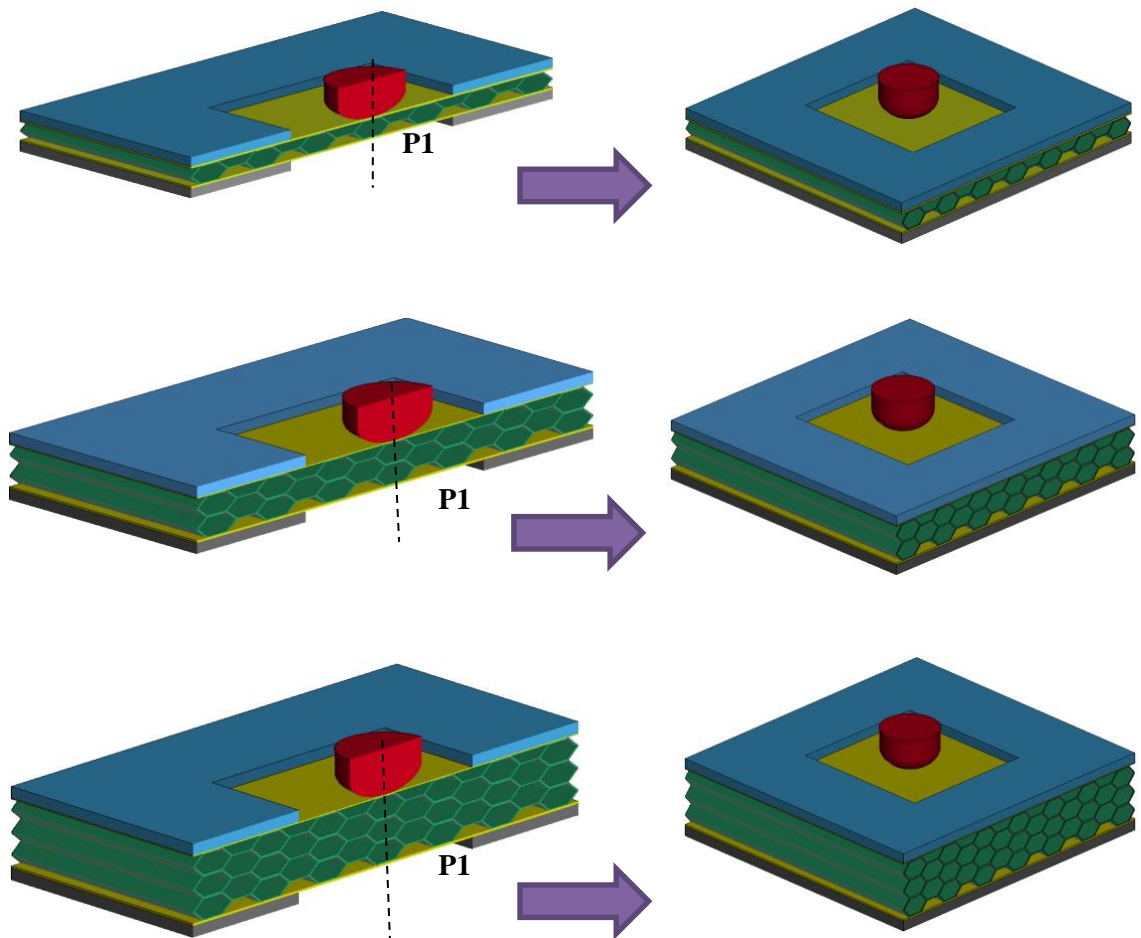


Figure 4. Impact points for P1.

An eight-node solid element (*ELFORM1*) was used in modeling. A total of 30197 nodes and 26750 solid elements were used. The diameter of the impactor is 20 mm and its weight is 5.5 kg. The lower and upper holders are modeled with 7740 nodes and 5500 solid elements. The upper and lower holders are fixed as in the experimental standards. Impactor can only move along the z axis. CONTACT AUTOMATIC SURFACE TO SURFACE contact card was used to keep the specimens between the upper and lower holders fixed and to ensure that it moves during impact, as in the experimental test subject. The CONTACT ERODING SURFACE TO SURFACE contact card was used between the impactor and the specimen. Static and dynamic friction coefficients on all contact cards are entered as 0.2 and 0.3, respectively [20].

A. 2. Modeling of adhesive layer

In sandwich composite structures, the core structure in the middle and the upper and lower face sheets must adhere to each other. This adhesion is achieved in the experimental laboratory by applying resin or adhesive materials such as *Araldite 55* to the contact surfaces. Some mechanical rules are adopted during the separation of these two structural elements connected to each other. In the literature, it is described as CZM with a bilinear tension-separation relationship. The basis of this law lies in the application of 3 independent parameters. The traction between the layers when the force is applied is t_0 , the separation distance that occurs when the damage begins is δ_0 and the remaining under this curve is G_c . After the impact occurs, separation between layers occurs according to this principle (Figure 5).

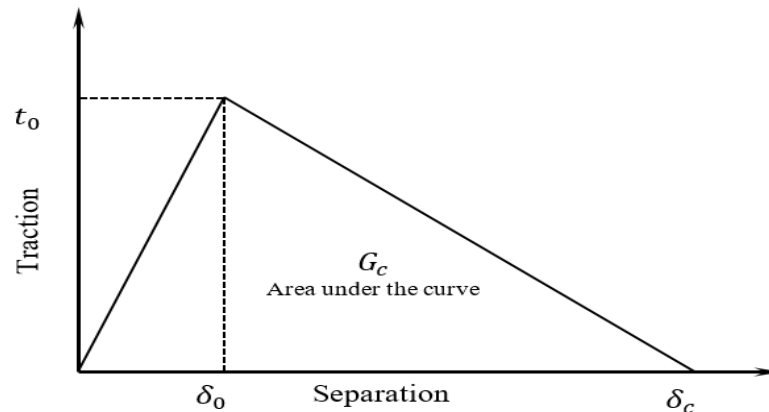


Figure 5. Bilinear traction-separation law.

Adhesion here can be achieved in two ways. This can be achieved by first defining a thin interface material between the top face sheets and the core in the middle. Or, this union can be achieved by using the adhesion surface that performs the same function. Dogan et al. [27] determined that this method is effective instead of using intermediate materials. In this study, *The CONTACT_AUTOMATIC SURFACE TO SURFACE TIEBREAK* contact card was used to adhere the upper and lower face sheets to the core material in between. While the adhesion here is achieved, as shown in Figure 5, separations occur based on the Bilinear tractionseparation law. With this contact card, the nodes making contact in the beginning connect with each other according to the following criterion. The condition for connecting the nodes here is applied according to this equation. When the equation equals 1, separation occurs.

$$\left(\frac{|\sigma_n|}{NFLS}\right)^2 + \left(\frac{|\sigma_s|}{SFLS}\right)^2 \geq 1 \quad (5)$$

Here, while σ_n and σ_s are the current normal and shear stresses, *NFLS* and *SFLS* are respectively the interface and shear strength. Mechanical properties of *Araldite 2015* are given in Table 2.

Table 2. Cohesive parameters of delamination between core and face sheets interfaces [25].

Contact Tiebreak Variable	Description	Value	Units
<i>NFLS</i>	Peak traction in normal direction	21.63x10 ⁹	Pa
<i>SFLS</i>	Peak traction in tangential direction	17.9x10 ⁹	Pa
<i>PARAM</i>	Exponent of mixed-mode criteria	1	-
<i>ERATEN</i>	Energy release rate for Mode I	430	N/m
<i>ERATES</i>	Energy release rate for Mode II	4700	N/m
<i>CT2CN</i>	Ratio of tangential stiffness to normal stiffness	1	-
<i>CN</i>	Normal stiffness	8080	Pa/m

A.3. Material Models

There are many material models that describe composite materials in the *LS DYNA* finite element program. The choice of these models varies depending on the purpose of use. *MAT-54* material model was used in this study. In this material model, fiber damage, matrix damage and delamination behavior under impact load can be determined based on the progressive damage principle. With this material model, *Hashin damage criteria* [28] are applied. A total of 24 parameters are required to introduce the *MAT-54* material model to the program. Details of these parameters are given in Table 3-4. The material of the core structure is determined as Aluminum 6061-T6. “*MAT 24 (PIECEWISE LINEAR ISOTROPIC PLASTICITY)*” material card was chosen to define this material in the *LS DYNA* finite element program. Mechanical properties of the materials used are given in Table 5.

Table 3. Mechanical parameters of the GFRP composite [5].

Symbol	Property	Value	Unit
ρ	Density	1500	kg/m ³
E_a, E_b	Young modulus <i>a</i> and <i>b</i> direction	19	GPa
E_c	Young modulus in <i>c</i> direction	6	GPa
ν_{ab}	Poisson’s ratio in <i>ab</i> plane	0.162	-
ν_{bc}	Poisson’s ratio in <i>bc</i> plane	0.162	-
ν_{ca}	Poisson’s ratio in <i>ca</i> plane	0.162	-
G_{ab}	Shear modulus in <i>ab</i> plane	3.786	GPa
G_{bc}	Shear modulus in <i>bc</i> plane	1.709	GPa
G_{ca}	Shear modulus in <i>ca</i> plane	1.709	GPa
S_{aT}	Tensile strength <i>a</i> direction	0.459	GPa
S_{aC}	Compressive strength <i>a</i> direction	0.2238	GPa
S_{bT}	Tensile strength <i>b</i> direction	0.459	GPa
S_{bC}	Compressive strength <i>b</i> direction	0.2238	GPa
S_{ab}	Shear strength in <i>ab</i> plane	0.0828	GPa

Table 4. Failure parameters of the GFRP composite [5].

Symbol	Description	Unit
<i>DFAILM</i>	Transverse matrix failure strain experimental	0.0
<i>DFAILS</i>	Shear failure strain experimental	0.0
<i>DFAILT</i>	Tensile fiber failure strain experimental	0.0
<i>DFAILC</i>	Compressive fiber failure strain experimental	0.0
<i>TFAIL</i>	Time step for element deletion computational	0.16
<i>Alpha</i>	Shear stress parameter damage dependent	0.0
<i>Soft</i>	Strength reduction factor damage dependent	0.7
<i>FBRT</i>	Reduction factor for X_t damage dependent	1
<i>YCFAC</i>	Reduction factor for X_c damage dependent	3
<i>EFS</i>	Efective failure strain computational	0.90

Table 5. Mechanical properties of Al 6061-T6.

Density (kg/m ³)	E (GPa)	Poisson ratio	Yield stress (MPa)	Failure strain
2850	72	0.33	252	0.4

A.4. MAT_54-55: Enhanced Composite Damage Model

It is the most commonly used material model in the analysis of composite structures. If there is no damage in the material model, the material is assumed to be orthotropic and linear elastic. In this model, *MAT 54* damage criterion was proposed by *Chang* and *MAT 55* damage criterion was proposed by *Tsai-Wu*. Although the working logic of this material model and the *MAT 22* model is the same, it additionally includes the compression damage mode. The *Chang–Chang* criterion (*MAT 54*) is given below;

Tensile fibre ($\sigma_{11} > 0$).

$$\left(\frac{\sigma_{11}}{s_1}\right)^2 + \bar{\tau} = 1 \quad (6)$$

All moduli and Poisson's ratios are set to zero when the tensile fibre failure criteria are met, that is $E_1 = E_2 = G_{12} = \nu_{12} = \nu_{21} = 0$ All the stresses in the elements are reduced to zero, and the element layer has failed.

Failure mode for compressive fibre ($\sigma_{11} > 0$),

$$\left(\frac{\sigma_{11}}{s_{12}}\right)^2 = 1 \quad (7)$$

Failure mode for tensile matrix ($\sigma_{11} > 0$),

$$\left(\frac{\sigma_{22}}{s_2}\right)^2 + \bar{\tau} = 1 \quad (8)$$

Failure mode for compressive matrix

$$\left(\frac{\sigma_{22}}{2S_{12}}\right)^2 + \left[\left(\frac{C_2}{2S_{12}}\right) - 1\right] \frac{\sigma_{22}}{C_2} + \bar{\tau} = 1 \quad (9)$$

Where E_1 and E_2 are the longitudinal and transverse elastic moduli, respectively, G_{12} is the shear modulus, ν_{12} and ν_{21} are the in-plane Poisson's ratios.

III. RESULTS AND DISCUSSION

Low-velocity impact simulations were carried out to determine the impact strength and damage behavior of aluminum core GRFP sandwich composite structures. At the end of the impact analysis, many graphs were obtained about the strength values of the material. An impact scenario can occur in three different ways, such as rebounding of the impactor from the specimen surface (rebounding), part or all of the impactor penetrating the specimen (penetration), and penetration of the impactor through the specimen (Perforation) [30]. In rebounding, there is energy returned elastically to the impactor, whereas in perforation and penetration, there is no energy returned elastically. During rebounding, the contact force returns to zero as the impactor retracts on the specimens surface. During penetration, the impact energy is completely absorbed by the specimen. But since there is still contact between the impactor and the specimen, it can be seen that there is a small force value. Force-Time, Force-Displacement, Absorbed energy-Time and Velocity-Time graphs for the velocities $V = 3, 5$ and 7 m/s of the sandwich specimen with face sheets thickness $t = 0.5$ mm are given in Figure 6. In the Contact force-Time graph in Figure 6a, the force reaches the maximum point due to the impactor contacting the specimen surface and then returns to the zero point with energy discharge. Here it is understood that the impactor rebounding back on the specimen surface and breaks contact with the specimen. In other words, it showed elastic properties here and a rebounding effect occurred. As the force reaches its peak point, it is seen that there are oscillations in the graphs for all three different velocities. Since damage occurs in the specimen layers with the impact, very small force decreases are experienced. Therefore, oscillations occur in the graph [18]. The maximum force value for velocities $V = 3, 5$ and 7 m/s was determined as 3.59 kN, 7.61 kN and 7.57 kN, respectively. In the impact test, it is expected that as the impact velocity increases, the contact force will also increase. But as damage occurs on the material, the contact force value decreases. Therefore, when the velocity of the impactor is 7 m/s, the contact force decreases because the specimen is damaged [[20],[30]].

In the Energy-Time graph in Figure 6b, impact tests were carried out with 9.88 J, 27.44 J and 53.78 J for $V = 3, 5$ and 7 m/s velocities, respectively. At the end of the impact test, the energies of the impactor were determined as 1.56 J, 2.50 J and 3.04 J, respectively. Here, when the remaining energy value is subtracted from the initial energy, the energy value absorbed by the specimen is obtained. By dividing the amount of absorbed energy by the initial energy, the absorbed energy value in % is obtained. This is called energy absorption efficiency [23]. At the end of the study, it will be used to compare the current study with the studies done in the literature. In the light of the information here, the energy absorption efficiency value is determined as 84.21% , 90.88% and 94.34% of the impact energy for velocities $V=3, 5$ and 7 m/s, respectively. In Figure 6c, it is seen in the graph that after full energy discharge occurs at the force peak value point, the force decreases to zero again and the impactor returns to the initial position. Here, the maximum displacement is determined as 5.6 mm for a velocity of $V= 7$ m/s. Figure 6d shows the change in the impactor's velocity. It is seen that the velocity decreases over time and remains constant after a point. When the graph is examined, it is seen that the impactor velocities change from positive to negative. Here the direction of the impactor is assigned as $+z$. Since the impactor moved in the opposite direction of the z direction, that is, in the $-z$ direction, while returning from the specimen surface, it entered the negative area in the graph.

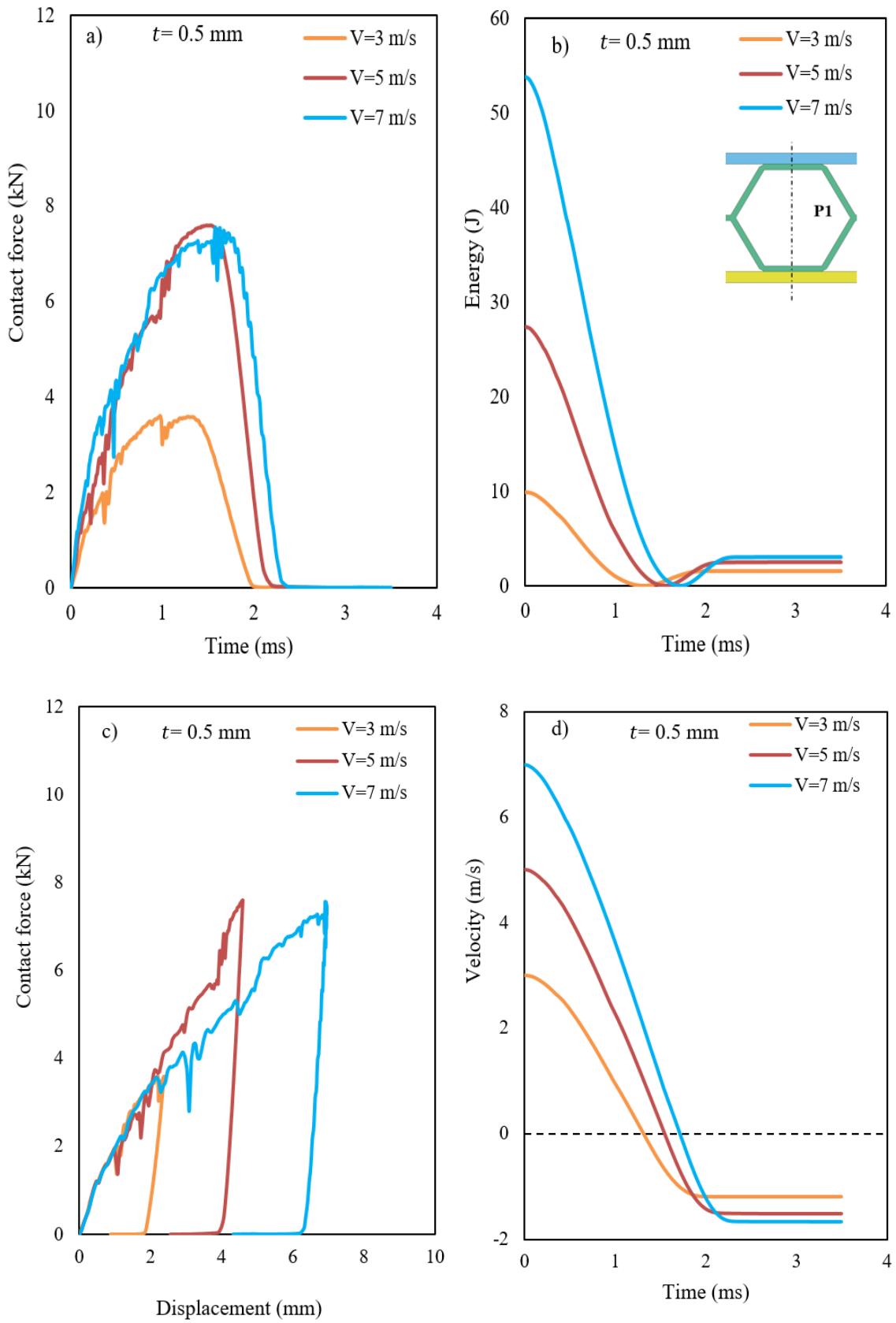


Figure 6. Variation of a) Contact force-Time, b) Energy-Time, c) Contact force-Displacement and d) Velocity-Time graphs with impact velocity ($t=0.5$ mm)

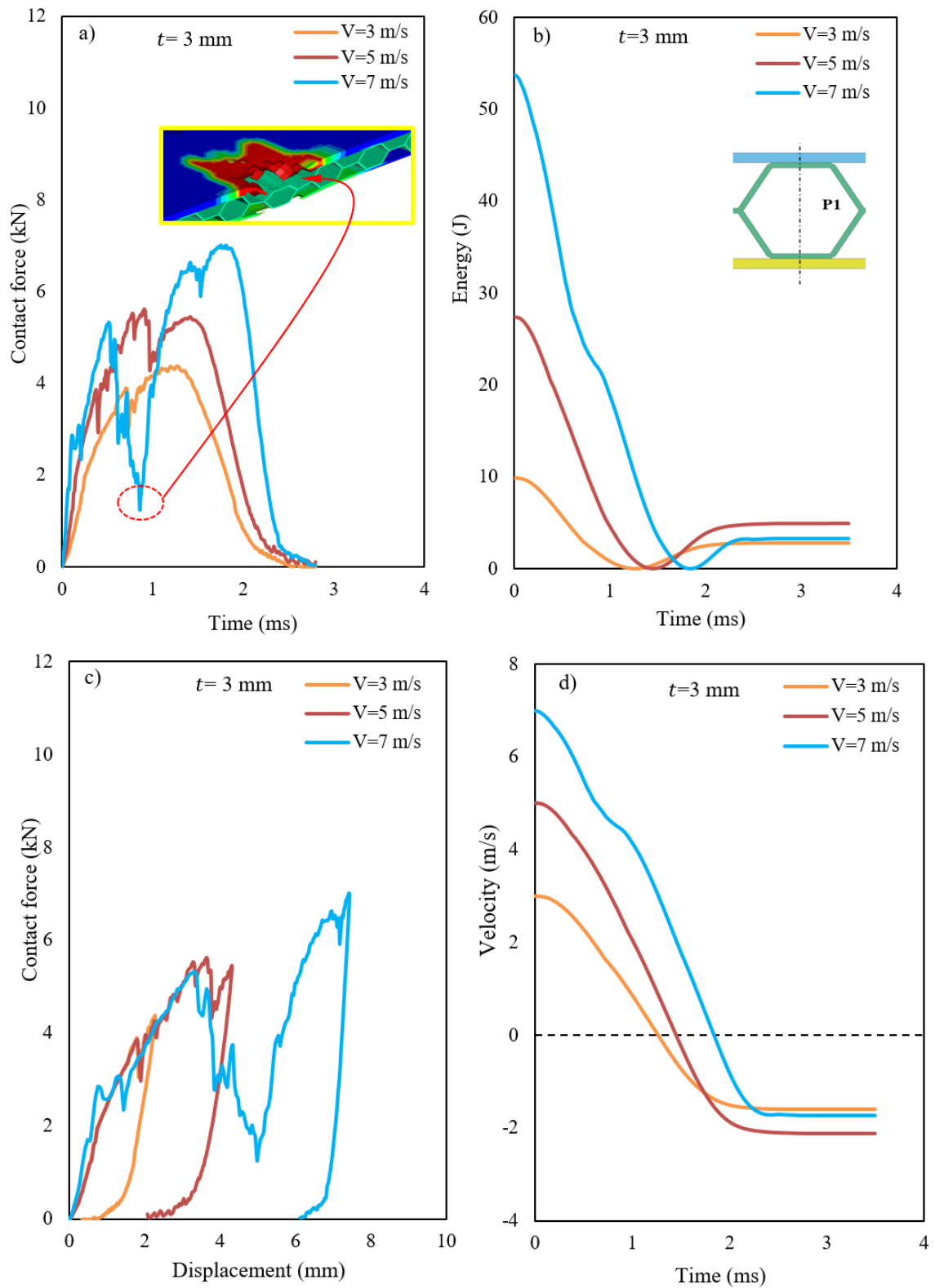


Figure 7. Variation of a) Contact force-Time, b) Energy-Time, c) Contact force-Displacement and d) Velocity-Time graphs with impact velocity ($t=3 \text{ mm}$).

It is important that all graphs are understandable and clear in order to better understand the behavior of material mechanics under load. Therefore, all graphics obtained during this research process were detailed and added to the study. Although it is known that the number of graphs and tables obtained in the study is large, it is important to use these graphs to show the material reaction for each changing parameter and to understand the material behavior at every second. When the studies in the literature are examined [[21], [30]], there is a similar approach.

Since similar scenarios were experienced for the velocities $V = 3, 5$ and 7 m/s of the sandwich specimen with face sheets thickness $t = 1$ and 1.5 mm, the details of these graphs were not detailed. However, in order to better understand and notice the effect of face sheet thickness, graphic details of the smallest and largest face sheets thickness measurements are given (Figure 6-7). As the face sheet thickness increases, the contact force value of the specimen also increases up to a point [31].

Since material rigidity increases with thickness, the composite face sheets may be damaged against impact load and this may show itself as a decrease in force on the graph [19]. In Figure 7, the strength values of the sandwich specimen with face sheets thickness $t = 3$ mm are given for velocities $V = 3, 5$ and 7 m/s. Figure 7a shows that the force drops sharply for $V = 7$ m/s and then increases again. The reason for this is that, due to the impact, the impactor penetrates the upper surface and reaches the core structure. With the breakage of the top face sheets, there was a decrease in the contact force. It should not be forgotten that the point where the impactor contacts is the P1 point. At this point, just below the top face sheets, there is a core structure that is adhesive with Araldite supporting it. Therefore, immediately after the top face sheets broke, the core structure underneath was also damaged. Then, after the impactor's energy reaches 0, the force also reaches 0.

Contact force and absorption energy vary depending on the impact intensity to which the composite structure is exposed. Figure 8 shows peak force and absorbed energy graphs for specimens with different thicknesses at $V = 3, 5$ and 7 m/s velocities. When calculating absorbed energy graphs, the amount of absorbed energy was obtained by dividing it by the initial amount of energy. When the value here reaches 1, it means that it has absorbed all of it. When the graph for $t=0.5$ in Figure 8a is examined, when the velocity of the impactor increases from 3m/s to 5m/s, the Peak force value increases by 1.108 times. When the impactor's velocity increased from 5 m/s to 7 m/s, it decreased by 0.54%, although it was expected to increase. Because there is a maximum value that the material can withstand. After this velocity value, the peak force value will not change no matter what velocity you hit. A4 paper can be given as an example. Even if the A4 paper is impact at 3 m/s or 5 m/s, the contact force value will not change much. Because after a certain impactor velocity, they will all penetrate. Therefore, the contact force will not change. In Figure 8b-c-d, it is seen that as the face sheet thickness increases, the contact force also increases. Since the maximum contact force values were not reached, it is seen that there is a parallelism between the thickness and the contact force [32]. When the impactor's velocity increases from 3 m/s to 5 m/s, the absorb energy value increases by 11.9%. This increase continues until a certain velocity value. From a certain point the material is penetrated to the boundary and at that point it reaches a value of 1. A value of 1 here means that the impact energy and the absorbed energy value are the same. When the graphs in Figure 8b-c-d are examined, it is seen that as the impactor velocity increases, the absorbed energy rate also increases [25].

The impact behaviors of 1-layer, 2-layers and 3-layers core structures were examined to determine the peak force and absorbed energy performance of the core structure, which is the main component of sandwich composite structures. The effect of the number of core layers on the peak force of specimens with face sheet thickness of 0.5 and 3 mm is given in Figure 9. When the specimen with a face sheet thickness of 0.5 was examined, the peak force value decreased by 7.18% when the number of core layers decreased from 1 to 3 (Figure 9a). In Figure 9b, in the specimen with 3 mm face sheet thickness, the number of core layers increased by 24.62% when the number of core layers increased from 1 to 3. Although the number of core layers increases at the same rate in two specimens with different face sheets thicknesses, peak force values are affected at different rates. It has been observed that the strength may not increase even though more core material is used. Therefore, it is

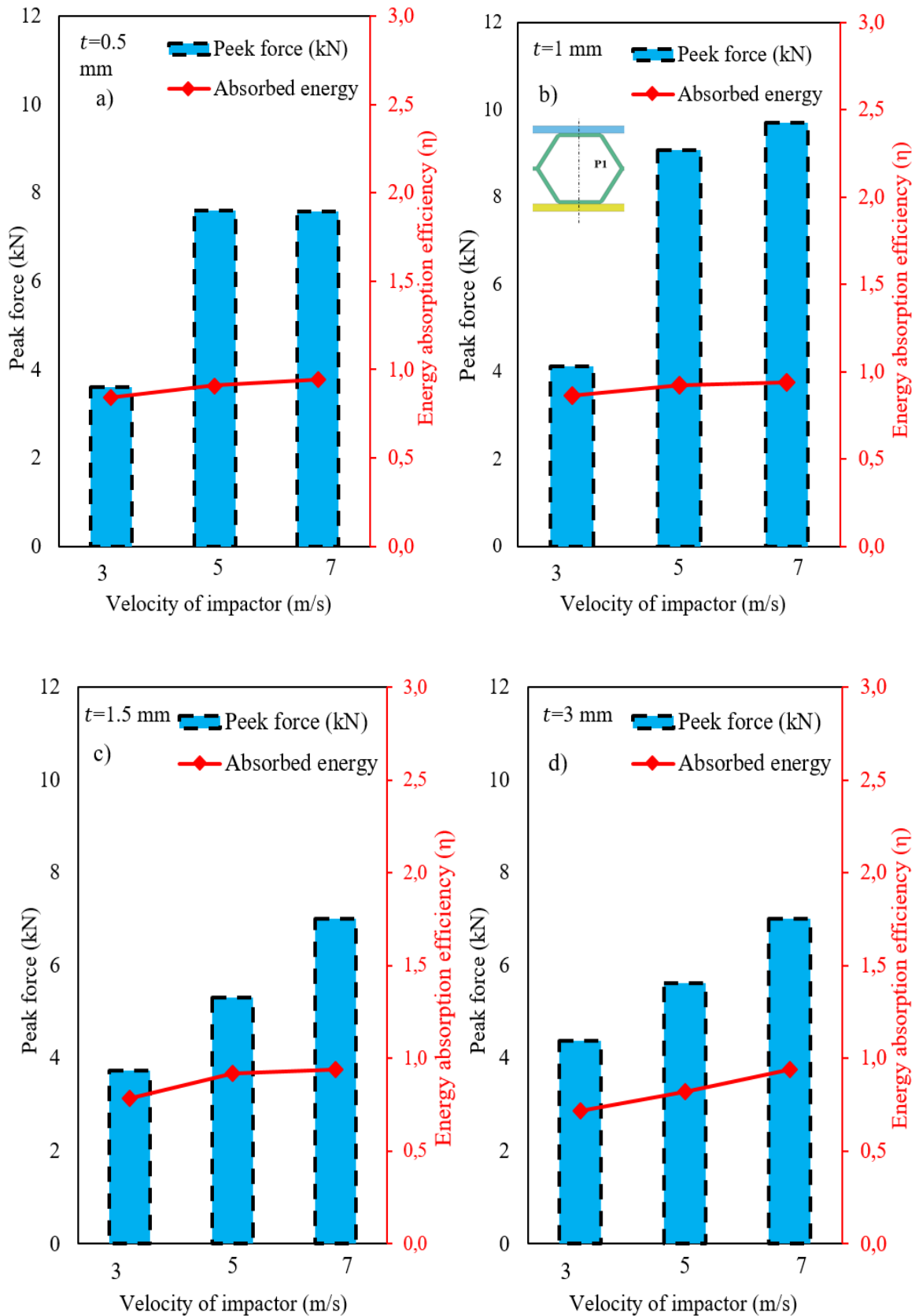


Figure 8. Effect of impactor velocity on peak force and absorbed energy variation for different face sheet.

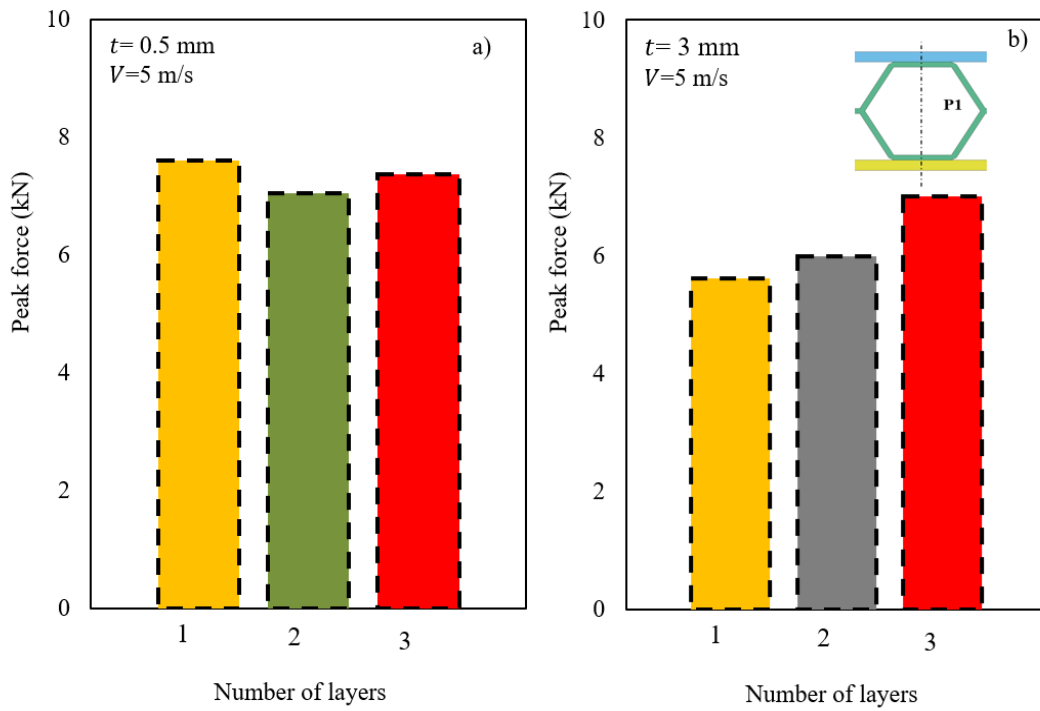


Figure 9. Effect of number of layers on peak force variation for a) $t=0.5$ mm and b) $t=3$ mm face sheet thickness.

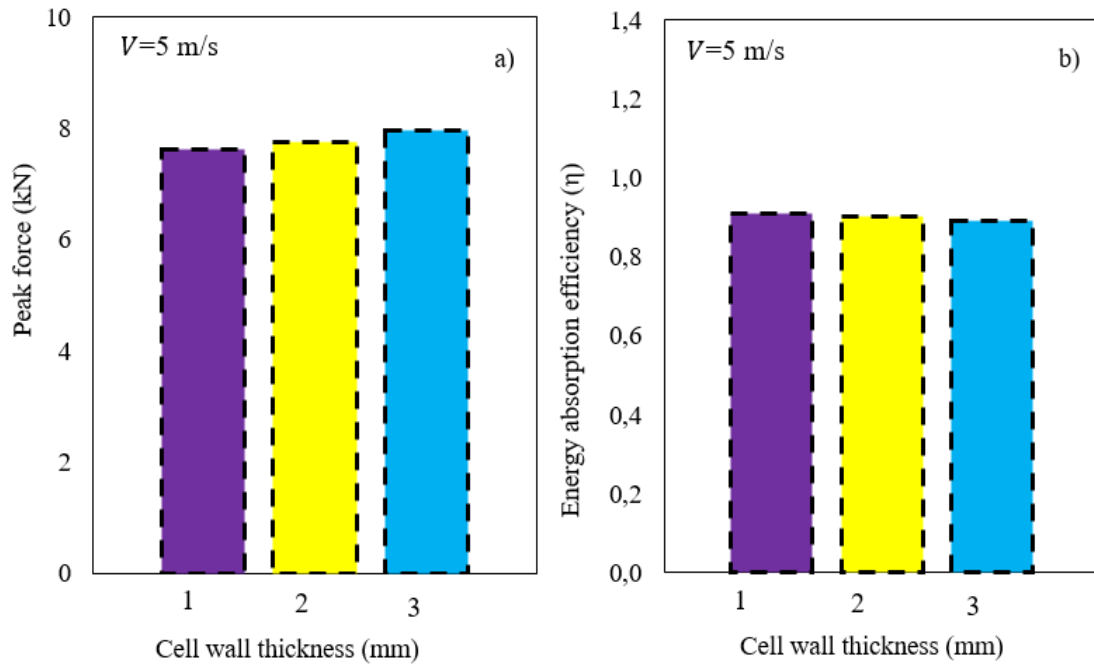


Figure 10. Effect of number of layers on peak force variation for a) $t=0.5$ mm and b) $t=3$ mm face sheet thickness.

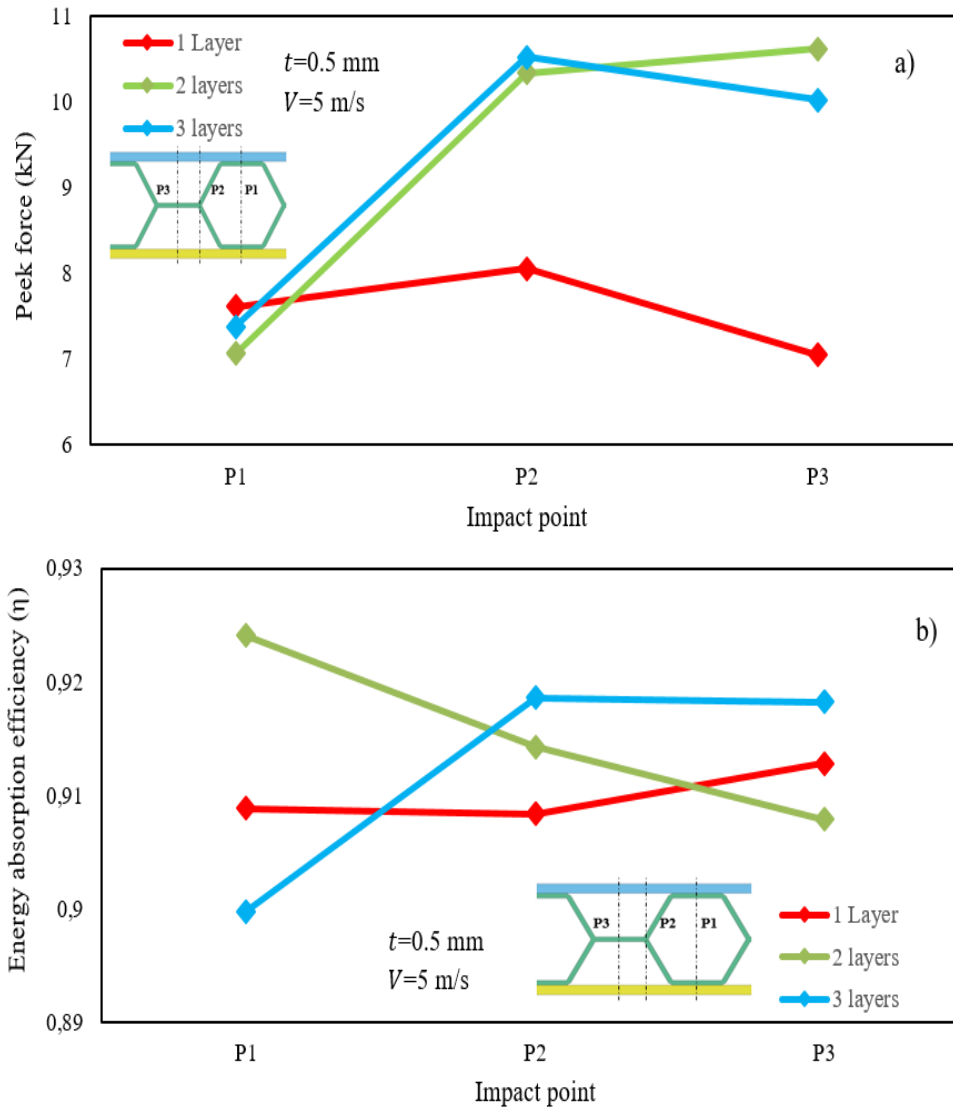


Figure 11. Peak force and Absorbed energy variation for different impact points.

very important that the face sheet thickness in sandwich structures is in harmony with the core structure and is determined correctly [20].

Another important parameter when designing sandwich composite structures is material thickness or cell wall thickness. A lot of research has been done on this parameter while preserving the principle of lightness, which is the main reason for using sandwich structures. The answer to the question of what the optimum cell wall is is not exactly clear. Because it must be determined what kind of loads

the area or component in which the sandwich composite structure is used should have. If the cell wall is designed accordingly, a more effective design will be made. In this study, 3 different cases with cell wall thickness of 0.5, 1 and 2 mm, respectively, are given in Figure 10. When the graph is examined, if the cell wall is increased from 0.5 mm to 2 mm, the peak force value increases by 1.87%. The energy absorption value decreases by 0.87%. Even though the energy absorption value decreased slightly as a percentage, there was an increase in the peak force value. Researchers decide whether it is necessary to build the system more heavily by using more materials for such an increase, by looking at the cost-benefit analysis. This decision is evaluated according to the area in which it is used. If necessary, this thickness can be added.

It may not be known at what point and at what intensity the impact will impact the sandwich composite structure. While designing, it should be done according to the worst case scenario and all situations should be evaluated. In this study, impact scenarios were applied for three different situations. Peak force and absorb energy values for these three different points are given in Figure 11. When Figure 11a is examined, in the specimens with the number of core layers 1, 2 and 3, the peak force values at point P1 were determined as 7.61 kN, 7.06 kN and 7.37 kN, respectively, at points P2 and P3. It was determined that the peak force value at the P2 point for all three specimens increased by 8.88%, 46.32% and 42.6%, respectively, reaching 8.05 kN, 10.33 kN and 10.52 kN. However, at P3 point, the peak force value in the specimen with 2 core layers increased by 2.25% compared to P2, while the peak force value decreased in the other two specimens. Whether the impact point has an effect on energy absorption is also examined in Figure 11b. In the sandwich specimen with a single layer core, if the impactor applies impact to P2 and P3 points instead of P1, the amount of energy absorption decreases by 0.06% and 0.49%, respectively. In the specimen with a 2-layer core, these values decrease by 1.06% and 0.7% for the P2 and P3 points, respectively. In the 3-layer core specimen, unlike the others, the energy absorption value for the P2 point increased by 2.1%.

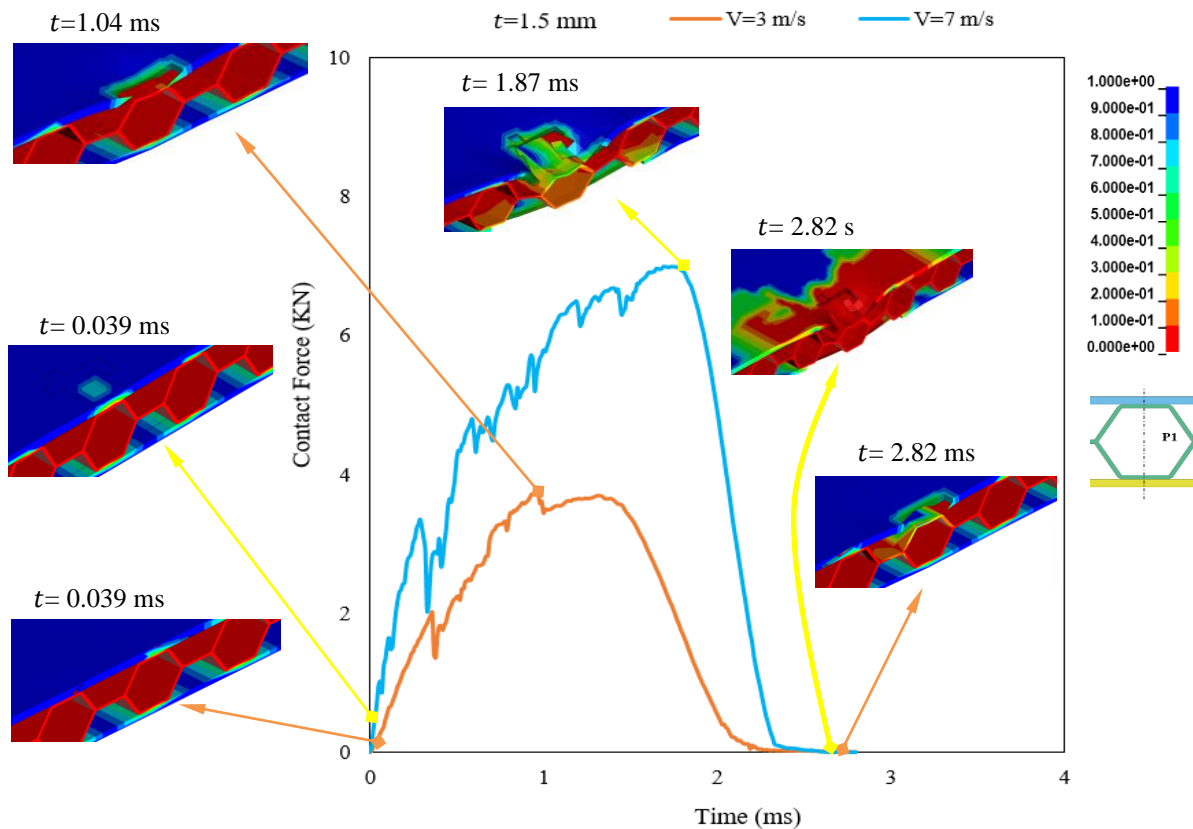


Figure 12. Matrix damage images of the 1.5 mm specimens.

Impactor produces graphics that provide information about the mechanics of the material from the moment the sandwich composite comes into contact with the sample. At each point of these graphs, information can be obtained about the deformation and strength of the material. In Figure 12, two different graphs of $V = 3$ m/s and 7 m/s are given for the specimen with a face sheet thickness of 1.5 mm. Material deformation images at the same contact moments are shown in both graphs. In this way, material deformations can be compared at certain points. Shortly after the striking sandwich contacted the specimen, the force started to increase and the stress values increased in both graphs for $t = 0.039$ ms. Both graphs reached peak values at different times. However, for $V = 6$ m/s, the

number and intensity of the oscillations that occur when reaching the peak value are higher. Because after contacting with high velocity and therefore high energy, the composite structure will want to absorb this energy [33]. In the graph that reached the peak force value at $t = 1.87$ ms, it was determined that the upper face sheet was broken and crushing damage occurred in the core structure. For $V = 3$ m/s, the peak value reached at $t = 1.04$ ms and it is seen that the upper face sheet was relatively damaged at this second and this damage reached the core. After the impactor's energy reaches 0, the contact force decreases to 0 and the impact ends. When the damage images at $t = 2.82$ ms were examined for both graphs, it was determined that more damage occurred at high velocity and progressed to crushing in the core structure.

Composite structures resort to damage types such as matrix cracking, fiber breakage or delamination in order to absorb the energy they are exposed to. In composite structures, the matrix absorbs the load first [34]. Therefore, the first structure to be damaged upon impact is the matrix. The function of the matrix is to hold the fibers together and distribute the incoming load to the fibers and therefore to the entire system. While performing this task, it is first exposed to damage. If the incoming load is high, it passes to other layers. Therefore, delamination damages are seen here. Delamination is the breakage that occurs in the matrix-rich region between layers with different fiber orientations. The most important cause of delamination; Differences in the bending stiffness of the layers due to different fiber orientations between the layers and bending-induced stresses [18]. Fibers are the strongest component of the structure. If the fibers break, the structure damage process is completed and the structure is damaged [20].

Finite element method is an analysis method frequently used to solve engineering problems. Especially in mechanical problems, results very close to the real values can be obtained in determining the critical points of structures or components under load or in determining damage morphologies [35]. Table 6 and Table 7 show separately the Tensile fiber mode, Compressive fiber mode, Tensile matrix mode and Compressive matrix mode of the specimens with $t=0.5$ mm and 3 mm face sheet specimen thicknesses, respectively. The regions shown here in red are the damaged areas, and the regions shown in blue are the regions where no damage occurs. Damage images were added by giving the surface in contact with the impactor, the back surface of the specimen, and the cross-section of the specimen in the thickness direction. The damages here occur according to the *Hashin damage criterion* [28], which examines damage situations in composite structures. Therefore, it is different and more complicated than the *yield criteria*, which examine the damage states of metals. When Table 6 is examined, it is seen that as the velocity of the impactor increases, the area of the damaged area on the specimen surface increases [36]. For all three velocity conditions, the most damage occurred in the Tensile matrix mode [37]. When $V = 3$ m/s, no Tensile fiber mode and Compressive fiber mode damage occurred on the back surface. However, it is seen that as the velocity value increases, these types of damage also occur. The impactor breaks the upper face sheet and causes crushing damage to the core structure. As the impactor velocity increases, the core structure puts pressure on the lower face sheet and damages it [38]. Table 7 shows that since the face sheets thickness is 3 mm, which is thicker, there is no damage to the back surfaces at $V = 3$ and 5 m/s. When the velocity value reached 7, damage started to occur on the back surface.

In aluminum core sandwich composite structure, the damage status of the core after impact is as important as the composite structure. The *Von Mises stress* distribution of the core, which helps absorb most of the energy, is given in Table 8. As the specimen thickness increases, the high stress area caused by impact decreases [39]. Since the stress value did not reach the yield point, no damage occurred to the structure. It is seen that deformations occur along with shape changes due to stress.

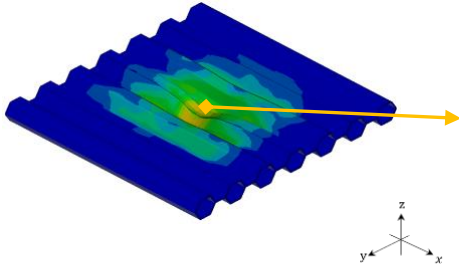
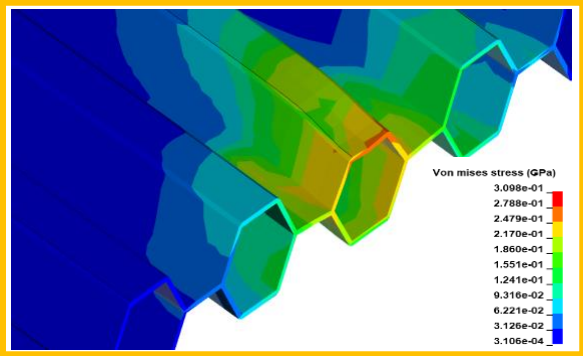
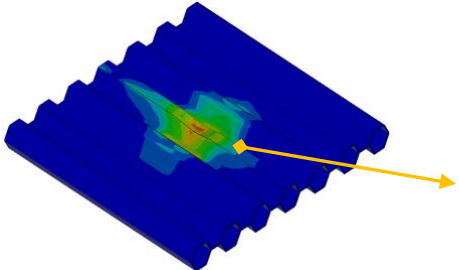
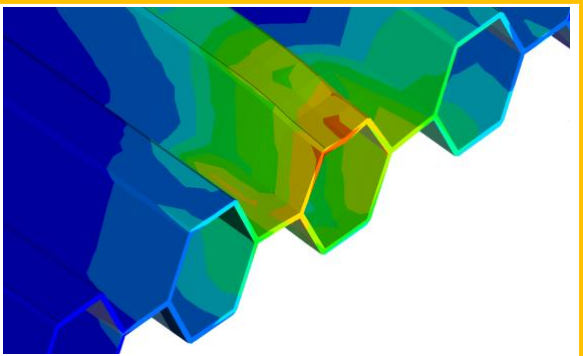
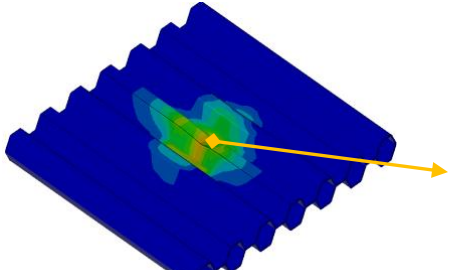
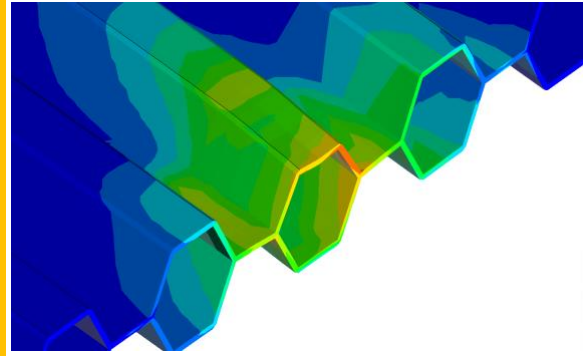
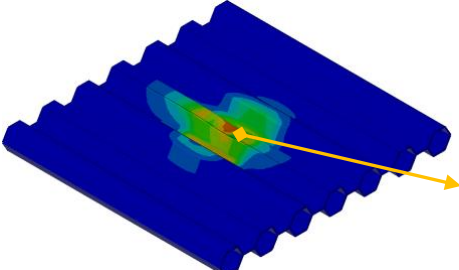
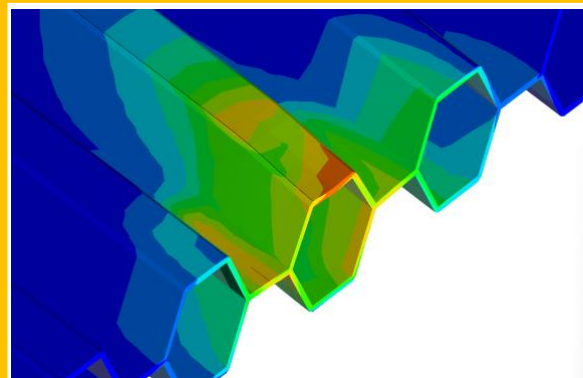
Table 6. Deformation images under impact force ($t = 0.5 \text{ mm}$).

$V \text{ (m/s)}$		Tensile fiber mode	Compressive fiber mode	Tensile matrix mode	Compressive matrix mode	Fringe levels
3	Top face					
	Back face					
	Section view					
5	Top face					
	Back face					
	Isometric					
7	Top face					
	Back face					
	Isometric					

Table 7. Deformation images under impact force ($t=3$ mm).

V (m/s)		Tensile fiber mode	Compressive fiber mode	Tensile matrix mode	Compressive matrix mode	Fringe levels
3	Top face					
	Back face					
	Section view					
5	Top					
	Back face					
	Isometric					
7	Top					
	Back face					
	Isometric					

Table 8. Impact damage areas of AL Core ($V=3$ m/s).

t (mm)	Damage area	
0.5		
1		
1.5		
3		

Comparing the efficiency of sandwich composite structures, which stand out with their energy absorption capacity, is evaluated by obtaining energy absorption efficiency values. The absorption efficiency values of the sandwich structures used in the current study were compared with other studies in the literature with different features and different structures [[23], [24], [36], [40]] (Figure 13). In the current study, the highest energy efficiency value was found in He et al. It is 3% less than the study by [23], Xue et al. It was determined to be 32% higher than the study conducted by [24]. The important thing here is to determine the optimum dimensions in terms of engineering by knowing the usage area of the sandwich composite structure and the load it will be exposed to. The focus of all these researches is to obtain the optimum design within minimum cost and maximum safety limits.

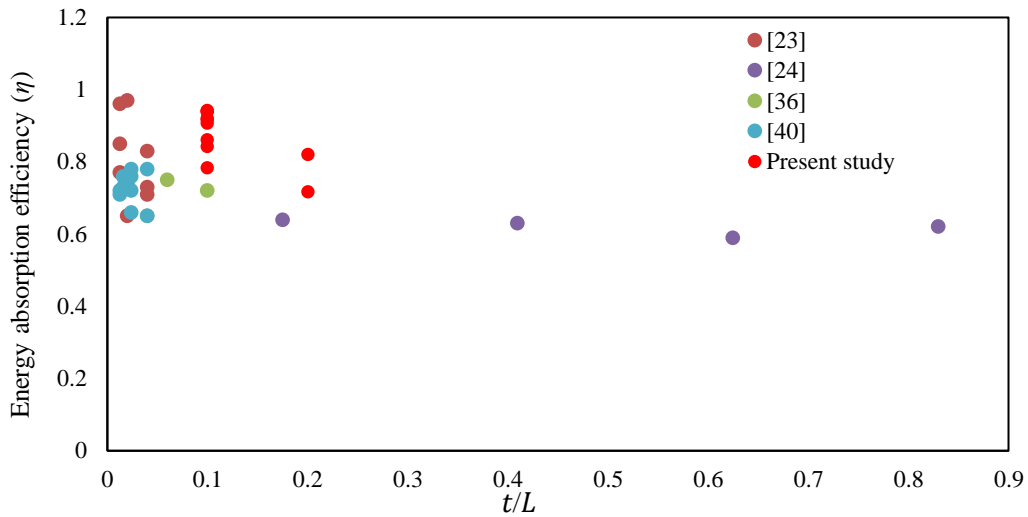


Figure 13. Comparison of energy absorption efficiencies.

IV. CONCLUSION

In this study, the low velocity impact behavior of aluminum honeycomb sandwich structures with fiber reinforced plastic (GFRP) face sheets was examined by the finite element method. In the study, low velocity impact tests were carried out in the *LS DYNA* finite element program to examine the effects of face sheet thickness, core number, wall thickness, impact location and impact velocity on maximum contact force, energy absorption efficiency and damage mode. Progressive damage analysis based on *Hashin damage criterion* and combination of *Cohesive Zone Model (CZM)* and the bilinear traction-separation law was performed using the *MAT-54* material model. Based on the data obtained at the end of the study, the results can be summarized as follows:

- When the result graphs were compared, it was seen that as the thickness of the face sheets increased, the peak contact force and initial hardness also increased. It has been determined that as the impact velocity gradually increases, there is a decrease in the contact force after a certain threshold value.
- As the impactor velocity increases, the energy absorption efficiency increases for all specimens.
- As the cell wall thickness increases, peak force and energy absorption efficiency values also increase.
- It has been determined that the location of the impact is very effective on peak force and energy absorption efficiency. The main reason for this is that the core structure consists of a hollow structure.

- The effect of the number of core layers depends on the face sheets thickness. It was determined that when the face sheets thickness was not damaged at first contact, the peak force value increased in parallel with the number of layers.
- The dominant post-impact damage mode was matrix damage, regardless of surface sheet thickness. It has been observed that as the energy level of the impactor increases, damage also occurs on the back surfaces. It has been noticed that this effect causes damage to the fibers, even leading to breakage.
- In the core structure, plastic buckling and higher stress conditions were determined at the points where the impactor contacts. It was observed that more crushing and plastic collapse damage occurred in the core structure in specimens with relatively thinner face sheets thickness.
- This can be supported by experimental work in future studies using the finite element model.

V. REFERENCES

- [1] Y. Rong, J. Liu, W. Luo, and W. He, “Effects of geometric configurations of corrugated cores on the local impact and planar compression of sandwich panels,” *Compos B Eng*, vol. 152, no. August, pp. 324–335, 2018, doi: 10.1016/j.compositesb.2018.08.130.
- [2] W. He, J. Liu, B. Tao, D. Xie, J. Liu, and M. Zhang, “Experimental and numerical research on the low velocity impact behavior of hybrid corrugated core sandwich structures,” *Compos Struct*, vol. 158, pp. 30–43, 2016, doi: 10.1016/j.compstruct.2016.09.009.
- [3] J. Liu, W. He, D. Xie, and B. Tao, “The effect of impactor shape on the low-velocity impact behavior of hybrid corrugated core sandwich structures,” *Compos B Eng*, vol. 111, pp. 315–331, 2017, doi: 10.1016/j.compositesb.2016.11.060.
- [4] Y. Hu, W. Li, X. An, and H. Fan, “Fabrication and mechanical behaviors of corrugated lattice truss composite sandwich panels,” *Compos Sci Technol*, vol. 125, pp. 114–122, 2016, doi: 10.1016/j.compscitech.2016.02.003.
- [5] I. Bozkurt, M. O. Kaman, and M. Albayrak., “LS-DYNA MAT162 Finding Material Inputs and Investigation of Impact Damage in Carbon Composite Plates. XVI. international research conference 2022.,” 2022.
- [6] A. Chinnarasu and K. Ramajeyathilagam, “Numerical study on influence of target thickness on impact response of GFRP composites,” *Mater Today Proc*, Jan. 2023, doi: 10.1016/j.matpr.2023.01.201.
- [7] A. Kurşun, M. Şenel, and H. M. Enginsoy, “Experimental and numerical analysis of low velocity impact on a preloaded composite plate,” *Advances in Engineering Software*, vol. 90, pp. 41–52, 2015, doi: 10.1016/j.advengsoft.2015.06.010.
- [8] F. Islam, R. Caldwell, A. W. Phillips, N. A. S. John, and B. G. Prusty, “A review of relevant impact behaviour for improved durability of marine composite propellers,” *Composites Part C: Open Access*, p. 100251, 2022, doi: 10.1016/j.jcomc.2022.100251.

- [9] S. Li, X. Li, Z. Wang, G. Wu, G. Lu, and L. Zhao, "Sandwich panels with layered graded aluminum honeycomb cores under blast loading," *Compos Struct*, vol. 173, pp. 242–254, Aug. 2017, doi: 10.1016/J.Compstruct.2017.04.037.
- [10] T Zhao, Y Jiang, Y Zhu, Z Wan, D Xiao, Y Li, H Li, C Wu, D Fang., "An experimental investigation on low-velocity impact response of a novel corrugated sandwiched composite structure," *Compos Struct*, vol. 252, no. June, p. 112676, 2020, doi: 10.1016/j.compstruct.2020.112676.
- [11] J. Zhang, K. Liu, Y. Ye, and Q. Qin, "Low-velocity impact of rectangular multilayer sandwich plates," *Thin-Walled Structures*, vol. 141, no. April, pp. 308–318, 2019, doi: 10.1016/j.tws.2019.04.033.
- [12] A. Manes, A. Gilioli, C. Sbarufatti, and M. Giglio, "Experimental and numerical investigations of low velocity impact on sandwich panels," *Compos Struct*, vol. 99, pp. 8–18, 2013, doi: 10.1016/j.compstruct.2012.11.031.
- [13] S. H. Abo Sabah, A. B. H. Kueh, and N. M. Bunnori, "Failure mode maps of bio-inspired sandwich beams under repeated low-velocity impact," *Compos Sci Technol*, vol. 182, no. February, p. 107785, 2019, doi: 10.1016/j.compscitech.2019.107785.
- [14] A. Akatay, M. Ö. Bora, O. Çoban, S. Fidan, and V. Tuna, "The influence of low velocity repeated impacts on residual compressive properties of honeycomb sandwich structures," *Compos Struct*, vol. 125, pp. 425–433, 2015, doi: 10.1016/j.compstruct.2015.02.057.
- [15] C. C. Foo, L. K. Seah, and G. B. Chai, "Low-velocity impact failure of aluminium honeycomb sandwich panels," *Compos Struct*, vol. 85, no. 1, pp. 20–28, Sep. 2008, doi: 10.1016/J.Compstruct.2007.10.016.
- [16] X. Li, P. Zhang, Z. Wang, G. Wu, and L. Zhao, "Dynamic behavior of aluminum honeycomb sandwich panels under air blast: Experiment and numerical analysis," *Compos Struct*, vol. 108, no. 1, pp. 1001–1008, Feb. 2014, doi: 10.1016/J.Compstruct.2013.10.034.
- [17] V. Crupi, G. Epasto, and E. Guglielmino, "Collapse modes in aluminium honeycomb sandwich panels under bending and impact loading," *Int J Impact Eng*, vol. 43, pp. 6–15, May 2012, doi: 10.1016/J.Ijimpeng.2011.12.002.
- [18] W. He, J. Liu, S. Wang, and D. Xie, "Low-velocity impact response and post-impact flexural behaviour of composite sandwich structures with corrugated cores," *Compos Struct*, vol. 189, no. January, pp. 37–53, 2018, doi: 10.1016/j.compstruct.2018.01.024.
- [19] W. He, J. Liu, S. Wang, and D. Xie, "Low-velocity impact behavior of X-Frame core sandwich structures – Experimental and numerical investigation," *Thin-Walled Structures*, vol. 131, no. July, pp. 718–735, 2018, doi: 10.1016/j.tws.2018.07.042.
- [20] I. Bozkurt, M. O. Kaman, and M. Albayrak, "Low-velocity impact behaviours of sandwiches manufactured from fully carbon fiber composite for different cell types and compression behaviours for different core types," *Materialpruefung/Materials Testing*, vol. 65, no. 9, pp. 1349–1372, 2023, doi: 10.1515/mt-2023-0024.
- [21] M. Albayrak, M. O. Kaman, and I. Bozkurt, "The effect of lamina configuration on low-velocity impact behaviour for glass fiber/rubber curved composites," *J Compos Mater*, vol. 57, no. 11, pp. 1875–1908, 2023, doi: 10.1177/00219983231164950.

- [22] M. Albayrak, M. O. Kaman, and I. Bozkurt, “Determination of LS-DYNA MAT162 Material Input Parameters for Low Velocity Impact Analysis of Layered Composites,” pp. 39–43, 2022.
- [23] W. He, L. Yao, X. Meng, G. Sun, D. Xie, and J. Liu, “Effect of structural parameters on low-velocity impact behavior of aluminum honeycomb sandwich structures with CFRP face sheets,” *Thin-Walled Structures*, vol. 137, no. August 2018, pp. 411–432, 2019, doi: 10.1016/j.tws.2019.01.022.
- [24] X. Xue, C. Zhang, W. Chen, M. Wu, and J. Zhao, “Study on the impact resistance of honeycomb sandwich structures under low-velocity/heavy mass,” *Compos Struct*, vol. 226, no. May, p. 111223, 2019, doi: 10.1016/j.compstruct.2019.111223.
- [25] I. Bozkurt, M. O. Kaman, and M. Albayrak, “Experimental and numerical impact behavior of fully carbon fiber sandwiches for different core types,” *Journal of the Brazilian Society of Mechanical Sciences and Engineering*, vol. 46, no. 5, p. 318, May 2024, doi: 10.1007/s40430-024-04865-3.
- [26] H. JO., LS-DYNA Keyword User’s Manual Volume II Material Models, Version 971. Livermore Software Technology Corporation; . [24]. 2017.
- [27] F. Dogan, H. Hadavinia, T. Donchev, and P. S. Bhonge, “Delamination of impacted composite structures by cohesive zone interface elements and tiebreak contact,” *Central European Journal of Engineering*, vol. 2, no. 4, pp. 612–626, 2012, doi: 10.2478/S13531-012-0018-0.
- [28] Z. Hashin, “Failure criteria for unidirectional fiber composites,” *Journal of Applied Mechanics, Transactions ASME*, vol. 47, no. 2, pp. 329–334, 1980, doi: 10.1115/1.3153664.
- [29] M. Albayrak and M. O. Kaman, “Production of Curved Surface Composites Reinforced With Rubber Layer,” *European Journal of Technic*, vol. 11, no. 1, pp. 19–22, 2021, doi: 10.36222/ejt.824761.
- [30] M. Albayrak, M. O. Kaman, and I. Bozkurt, “Experimental and Numerical Investigation of the Geometrical Effect on Low Velocity Impact Behavior for Curved Composites with a Rubber Interlayer,” *Applied Composite Materials*, vol. 30, no. 2, pp. 507–538, 2023, doi: 10.1007/s10443-022-10094-5.
- [31] V. Crupi, E. Kara, G. Epasto, E. Guglielmino, and H. Aykul, “Prediction model for the impact response of glass fibre reinforced aluminium foam sandwiches,” *Int J Impact Eng*, vol. 77, pp. 97–107, 2015, doi: 10.1016/j.ijimpeng.2014.11.012.
- [32] C. C. Foo, L. K. Seah, and G. B. Chai, “Low-velocity impact failure of aluminium honeycomb sandwich panels,” *Compos Struct*, vol. 85, no. 1, pp. 20–28, Sep. 2008, doi: 10.1016/J.Compstruct.2007.10.016.
- [33] İ. Bozkurt, M. Kaman, and M. Albayrak, “LS-DYNA MAT162 Finding Material Inputs and Investigation of Impact Damage in Carbon Composite Plates. XVI. international research conference 2022.,” pp. 3–7, 2022.
- [34] A Tarafdar, G Liaghat, H Ahmadi, O Razmkhah, SC Charandabi, MR Faraz, E Pedram., “Quasi-static and low-velocity impact behavior of the bio-inspired hybrid Al/GFRP sandwich tube with hierarchical core: Experimental and numerical investigation,” *Compos Struct*, vol. 276, p. 114567, Nov. 2021, doi: 10.1016/J.Compstruct.2021.114567.

- [35] B. M. Icten, B. G. Kiral, and M. E. Deniz, "Impactor diameter effect on low velocity impact response of woven glass epoxy composite plates," *Compos B Eng*, vol. 50, pp. 325–332, 2013, doi: 10.1016/j.compositesb.2013.02.024.
- [36] T. Boonkong, Y. O. Shen, Z. W. Guan, and W. J. Cantwell, "The low velocity impact response of curvilinear-core sandwich structures," *Int J Impact Eng*, vol. 93, pp. 28–38, 2016, doi: 10.1016/j.ijimpeng.2016.01.012.
- [37] JS Yang, WM Zhang, F Yang, SY Chen, R Schmidt, KU Schröder, L Ma, LZ Wu., "Low velocity impact behavior of carbon fibre composite curved corrugated sandwich shells," *Compos Struct*, vol. 238, no. August 2019, pp. 1–16, 2020, doi: 10.1016/j.compstruct.2020.112027.
- [38] Y. Chen, S. Hou, K. Fu, X. Han, and L. Ye, "Low-velocity impact response of composite sandwich structures: Modelling and experiment," *Compos Struct*, vol. 168, pp. 322–334, 2017, doi: 10.1016/j.compstruct.2017.02.064.
- [39] W. Shen, B. Luo, R. Yan, H. Zeng, and L. Xu, "The mechanical behavior of sandwich composite joints for ship structures," *Ocean Engineering*, vol. 144, no. July, pp. 78–89, 2017, doi: 10.1016/j.oceaneng.2017.08.039.
- [40] Y. Duan, Z. Cui, X. Xie, Y. Tie, T. Zou, and T. Wang, "Mechanical characteristics of composite honeycomb sandwich structures under oblique impact," *Theoretical and Applied Mechanics Letters*, vol. 12, no. 5, p. 100379, Sep. 2022, doi: 10.1016/J.Taml.2022.100379.